Bull Earthquake Eng (2017) 15:2853–2877
DOI 10.1007/s10518-016-0078-2

ORIGINAL RESEARCH PAPER

National-level prediction of expected seismic loss based on historical catalogue

Anna Bozza[1] · **Domenico Asprone**[1] · **Fatemeh Jalayer**[1] · **Gaetano Manfredi**[1]

Received: 1 October 2015 / Accepted: 23 December 2016 / Published online: 4 January 2017

Abstract The frequency and severity of natural catastrophes have increased significantly over the last few years, with countries around the world having to face huge economic and human losses. Italy in particular is very seismic-prone, being located in the precise area of convergence between the African and Eurasian lithospheric plates. In addition, most Italian cities are densely populated and have many old and historical buildings, making the country even more exposed and vulnerable in terms of potential losses. Recently, new regulations gave householders the chance to buy insurance against earthquakes. Unfortunately, the widespread risk perception in Italy is very low among the population. In addition, insurance premiums can be extremely high given the low-probability-high-risk of cash flow and insolvency problems potentially incurred by an insurance company if there is a high magnitude earthquake. The aim of the methodology proposed in this paper is to give insurers an engineering instrument with which to quantify expected losses in the case of an earthquake. This will enable insurance companies to model innovative and more affordable financial products by optimizing the quantification of premiums. Seismic events with a magnitude greater than 4 from 217 a.C. to 2012 have been selected from the historical catalogue of the National Institute of Geophysics and Volcanology, and statistical simulations of earthquake scenarios are performed for each of them. In particular, the peak ground acceleration is simulated, based on the ground motion prediction equation of Bindi et al. (Bull Earthq Eng 7(3):591–608, 2009). Actual exposure is assumed for the Italian

✉ Anna Bozza
anna.bozza@unina.it

Domenico Asprone
domenico.asprone@unina.it

Fatemeh Jalayer
fatemeh.jalayer@unina.it

Gaetano Manfredi
gaetano.manfredi@unina.it

[1] Department of Structures for Engineering and Architecture, University of Naples "Federico II", Via Claudio 21, 80125 Naples, Italy

building stock, which is modelled according to the database of the National Institute of Statistics. Finally, in order to compute the total losses for the entire national building stock, the annual expected losses are quantified according to the procedure demonstrated in Asprone et al. (Struct Saf 44:70–79, 2013).

Keywords Insurance industry · Loss assessment · PBEE · Earthquake scenario analysis

1 Introduction

Damage from natural events such as windstorms, earthquakes, storm surges and lightning causes economic losses amounting to billions of dollars throughout the world every year. Hurricane Sandy in 2012, for instance, caused losses of 19 billion dollars, while the earthquakes that occurred in New Zealand and Japan led to 2011 being a record year for catastrophic losses, with 380 billion dollars paid out, as estimated by Munich Re (2011).

It is clear from the world map of natural hazards below (Fig. 1) that natural risks threaten global and local communities more than ever, and are thus a source of great concern for national governments today.

Private insurance is widely recognized as a risk management strategy, which enables to transfer the risk. On the other hand, it is also true that risk mitigation strategies are constituted by a multiplicity of actions and instruments. In this view, private insurance can effectively be considered as a support instrument aiming at both transferring the risk but also to mitigate losses. Based on probability-based loss assessment models, in fact to date it is possible to forecast losses from catastrophes and to create dedicated funds for their coverage in case of a seismic event occurrence, preventing insurers from insolvency problems. Moreover, and particularly in Italy, catastrophe losses are often handled by public institutions and governments. Keeping with this, to date private insurance can be interpreted as one of the most effective ways to mitigate losses from natural disasters. Due to its high capability of transferring risk, it can be in fact considered as an instrument to mitigate public and also private house holders losses.

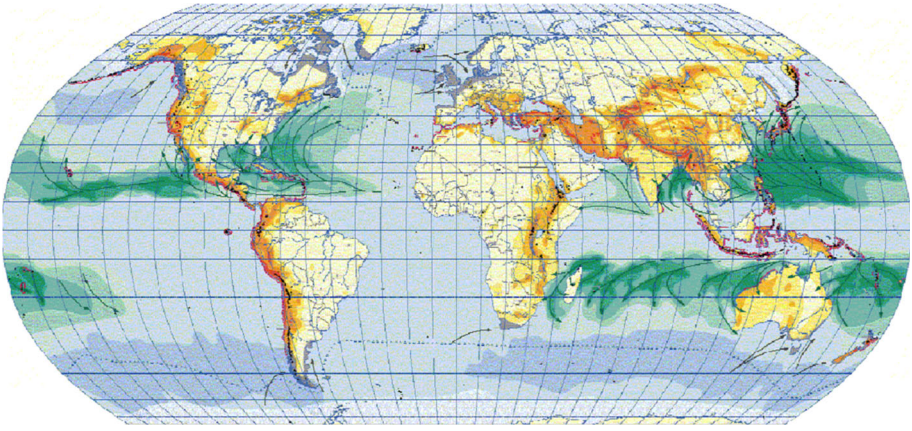

Fig. 1 World map of natural hazards, developed and updated by Munich Re (2011)

In this view, insurance has got the potential to encourage property owners to adopt risk reduction measures and support the management of catastrophe risks within urban environments.

Unfortunately, attempts to roll-out such insurance systems face a number of different problems, particularly when dealing with the private householder's market. Indeed, householders have a very low perception of risk and are risk adverse, i.e. they are unwilling to either spend their money on buying a product that will not necessarily provide value (insurance) or voluntarily adopt cost-effective protective measures (which can reduce insurance premiums). Consequently, they are often uninsured and do not invest in retrofits to prevent and mitigate the losses caused by natural disasters (Kesete et al. 2014).

Yet the risk is even higher for the insurance industry. Indeed, in the aftermath of a disaster, insurers are prone to insolvencies and significant destabilization. There are also problems due to the high risk of the industry exceeding its financial capacity and facing cash flow issues, all of which leads to very high insurance premiums.

Looking at the 10 costliest events that occurred from 1980 to 2014, it is notable that six of them were earthquakes (Fig. 2).

Italy is a particularly seismic-prone area, and has been affected by over 30,000 medium- and high-magnitude earthquakes in the last 2500 years. With this in mind, this study proposes predictive relationships for the actual expected losses given the magnitude of the occurred seismic event. This methodology has been developed to help communities to improve their capacity to withstand natural catastrophes like earthquakes. As most Italian earthquakes are due to the activity of faults, their locations and mechanisms can be, at least approximately, be predicted. As a consequence, it can be assumed that expected seismic events may be similar to those in the past and collected in the Italian historical catalogue produced by the National Institute of Geophysics and Volcanology (INGV 2004).

In this paper, a scenario analysis is performed of historical earthquakes with a magnitude greater than 4 within a full-scale study. Actual exposure is assumed by accounting for residential buildings located in each Italian municipality that is prone to experiencing seismic events. Total losses for the entire national building portfolio are then computed for each event, depending on the site-specific seismic hazard.

Date	Event	Affected area	Overall losses in US$ m original values	Insured losses in US$ m original values	Fatalities
11.3.2011	Earthquake, tsunami	Japan: Aomori, Chiba, Fukushima, Ibaraki, Iwate, Miyagi, Tochigi, Tokyo, Yamagata	**210,000**	40,000	15,880
25-30.8.2005	Hurricane Katrina, storm surge	USA: LA, MS, AL, FL	**125,000**	62,200	1,322
17.1.1995	Earthquake	Japan: Hyogo, Kobe, Osaka, Kyoto	**100,000**	3,000	6,430
12.5.2008	Earthquake	China: Sichuan, Mianyang, Beichuan, Wenchuan, Shifang, Chengdu, Guangyuan, Ngawa, Ya'an	**85,000**	300	84,000
23-31.10.2012	Hurricane Sandy, storm surge	Bahamas, Cuba, Dominican Republic, Haiti, Jamaica, Puerto Rico, USA, Canada	**68,500**	29,500	210
17.1.1994	Earthquake	USA: CA, Northridge, Los Angeles, San Fernando Valley, Ventura, Orange	**44,000**	15,300	61
1.8-15.11.2011	Floods	Thailand: Phichit, Nakhon Sawan, Phra Nakhon Si Ayuttaya, Pathumthani, Nonthaburi, Bangkok	**43,000**	16,000	813
6-14.9.2008	Hurricane Ike	USA, Cuba, Haiti, Dominican Republic, Turks and Caicos Islands, Bahamas	**38,000**	18,500	170
27.2.2010	Earthquake, tsunami	Chile: Concepción, Metropolitana, Rancagua, Talca, Temuco, Valparaíso	**30,000**	8,000	520
23.10.2004	Earthquake	Japan: Honshu, Niigata, Ojiya, Tokyo, Nagaoka, Yamakoshi	**28,000**	760	46

Source: Munich Re, NatCatSERVICE, 2015

Fig. 2 List of the 10 costliest events worldwide from 1980 to 2014 (Munich Re 2015)

The results are processed through a regression analysis to reveal the relationships between expected losses and magnitude. Furthermore, bin processing of the empirical results was also performed to highlight the most effective predictive curve for seismic loss assessments that can potentially be used by the insurance industry in Italy.

2 Supporting the insurance industry with a PBEE-based methodology

As a tool for the insurance industry, the methodology proposed in this paper uses an engineering-based instrument for the efficient and prompt forecasting of seismic losses on the basis of the magnitude of an expected seismic event.

Traditional, and often too conservative, practices concerning catastrophic losses can lead to the overestimation of premiums, and can thus be improved, with the result being more affordable insurance. The scenario analysis set out in this paper will ensure that more detailed knowledge of potential losses is available. As a result, insurers will be able to mitigate their insolvency risks, while reinsurers and governments can be involved in the interactions between insurers and property owners. The developed curves, in fact, can potentially enable insurers to forecast expected losses, based on the magnitude of the expected seismic events. Basically, each area has got a specific seismic hazard, from which the most probable earthquake intensity, hence its magnitude, which can be experienced can be known.

Insurers typically cannot guarantee for the full coverage of the insurance they sell, in case the insured event occurs. Furthermore, they can arrange for dedicated fund to cover losses in case of earthquake. But these are funds which mostly cannot cover losses from catastrophes. With this, insurers can in turn ensure for their capital safeguarding, through the purchase of reinsurance products.

Whether an insurer decide to buy reinsurance, this constitutes an additional cost, which will burden insurance premiums to be paid by home owners. In this case, local and/or national governments can be directly involved in the insurance process, to safeguard private owners and insurers, while contextually preventing from the collapse of the economic system in force. Synergy between private insurance company and governments can in fact potentially be very effective. For instance, insurers can sell insurance with certain maximum coverage and excess level. The excess enable for minor damages to be handled by private owners, and helping to limit the premiums' amount. On the other hand, maximum coverage enable insurers to protect their founds, and eventually this can be merged with the institution intervention. Governments can share losses with insurers in case of catastrophic seismic events, ensuring for an equitable distribution.

A realistic correlation between seismic effects at different locations and on multiple structures is considered when performing the scenario analysis. Indeed, a more accurate description of aggregate seismic losses is possible through the modelling of Italy's building stock as a spatially distributed system, with reference to each municipality (ISTAT 2011). Accordingly, the accumulation of seismic losses is also recognizable based on the seismic hazards faced by each site, as defined by the Italian seismic code.

Such a methodology also allows insurers to assess a type of region-specific loss ratio (Jaiswal and Wald 2013) that is based on historical earthquake characteristics and represents the seismic risk in a disaggregated manner. Expected direct losses are evaluated for actual assets, and a realistic correlation of seismic effects is modelled by taking into account two limit cases for the ground motion variability representation. Consequently, a

case in which there is partial correlation between, and variability among, the peak ground acceleration (PGA) values in each municipality was modelled, as is a case in which there is no correlation. Losses were then evaluated for each case and the results in terms of the predictive relationship of losses against magnitude are compared.

The procedure used to draw loss curves vis-a-vis magnitude is also described.

2.1 Ingredients to implement the methodology

The primary requirement for effectively implementing the methodology proposed in this paper is a database containing the details of all previous seismic events in the studied area.

To develop the proposed macro-economic-based approach, data on losses at diverse seismic intensities (in the present study the magnitude) are needed to examine the experimental relationship between loss and the intensity measure (IM). Such information is obtained by performing a scenario analysis based on historical earthquake data, although this information is rarely available for most historical seismic events worldwide (Jaiswal and Wald 2013).

Nonetheless, in Italy, the National Institute of Geophysics and Volcanology (INGV) and the Department of Civil Protection have developed a very precise database/catalogue that accounts for all previous seismic events in the country. In particular, this resource covers more than 1100 events from 217 b.C. to 2002 with a magnitude greater than 4.

The INGV catalogue (Fig. 3) provides a number of parameters that are fundamental for the implementation of the scenario analysis, such as the geographical coordinates of the epicentre and magnitude of each event.

It can be seen from the map that earthquakes with different magnitudes have been experienced throughout the Italian peninsula. As is well known, the seismic hazard levels in Italy, as well as the dominant earthquakes in terms of expected magnitude and damage, are different according to the area being examined. This is due to diverse local exposure and, above all, seismic hazard distribution, as shown in Fig. 4.

For instance, areas with higher seismic hazard are the Alps, the Apennines and the Calabrian arch. An example is the annual rate of seismic events experienced in diverse Italian municipalities over the return period of 475 years, which is a common probability

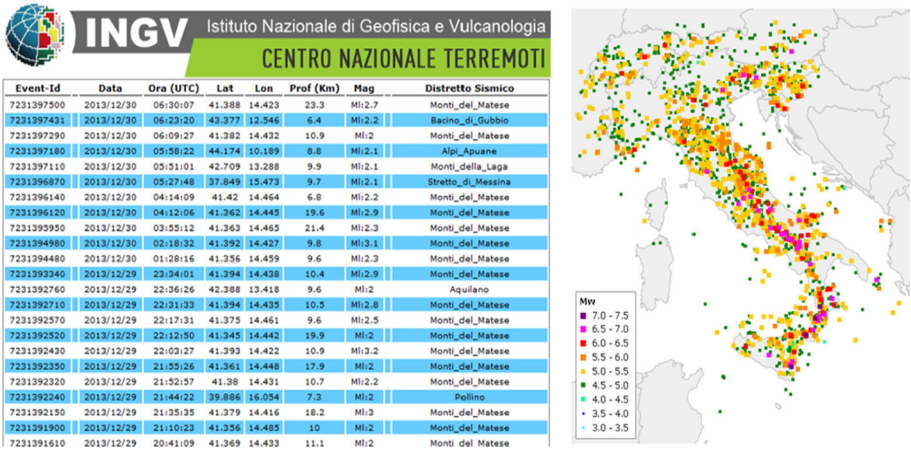

Event-Id	Data	Ora (UTC)	Lat	Lon	Prof (Km)	Mag	Distretto Sismico
7231397500	2013/12/30	06:30:07	41.388	14.423	23.3	Ml:2.7	Monti_del_Matese
7231397431	2013/12/30	06:23:20	43.377	12.546	6.4	Ml:2.2	Bacino_di_Gubbio
7231397290	2013/12/30	06:09:27	41.382	14.432	10.9	Ml:2	Monti_del_Matese
7231397180	2013/12/30	05:58:22	44.174	10.189	8.8	Ml:2.1	Alpi_Apuane
7231397110	2013/12/30	05:51:01	42.709	13.288	9.9	Ml:2.1	Monti_della_Laga
7231396870	2013/12/30	05:27:48	37.849	15.473	9.7	Ml:2.1	Stretto_di_Messina
7231396140	2013/12/30	04:14:09	41.42	14.464	6.8	Ml:2.2	Monti_del_Matese
7231396120	2013/12/30	04:12:06	41.362	14.445	19.6	Ml:2.9	Monti_del_Matese
7231395950	2013/12/30	03:55:12	41.363	14.465	21.4	Ml:2.3	Monti_del_Matese
7231394980	2013/12/30	02:18:32	41.392	14.427	9.8	Ml:3.1	Monti_del_Matese
7231394480	2013/12/30	01:28:16	41.356	14.459	9.6	Ml:2.3	Monti_del_Matese
7231393340	2013/12/29	23:34:01	41.394	14.438	10.4	Ml:2.9	Monti_del_Matese
7231392760	2013/12/29	22:36:26	42.388	13.418	9.6	Ml:2	Aquilano
7231392710	2013/12/29	22:31:33	41.394	14.435	10.5	Ml:2.8	Monti_del_Matese
7231392570	2013/12/29	22:17:31	41.375	14.461	9.6	Ml:2.5	Monti_del_Matese
7231392520	2013/12/29	22:12:50	41.345	14.442	19.9	Ml:2	Monti_del_Matese
7231392430	2013/12/29	22:03:27	41.393	14.422	10.9	Ml:3.2	Monti_del_Matese
7231392350	2013/12/29	21:55:26	41.361	14.448	17.9	Ml:2	Monti_del_Matese
7231392320	2013/12/29	21:52:57	41.38	14.431	10.7	Ml:2.2	Monti_del_Matese
7231392240	2013/12/29	21:44:22	39.886	16.054	7.3	Ml:2	Pollino
7231392150	2013/12/29	21:35:35	41.379	14.416	18.2	Ml:3	Monti_del_Matese
7231391900	2013/12/29	21:10:23	41.356	14.485	10	Ml:2	Monti_del_Matese
7231391610	2013/12/29	20:41:09	41.369	14.433	11.1	Ml:2	Monti del Matese

Fig. 3 The Italian historical catalogue of earthquakes from INGV (INGV 2004)

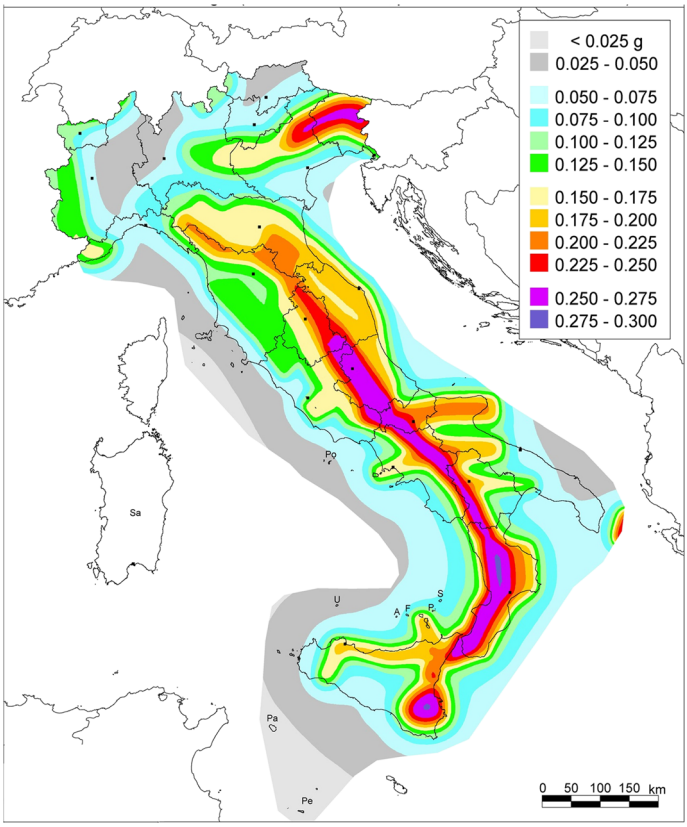

Fig. 4 Map of seismic hazards for the Italian peninsula (OPCM 3519—2006); 10% probability of exceedance in 50 years

level examined for seismic risk management. The expected PGA is equal to 0.25 g for the city of Messina (Calabrian arch), 0.26 g for L'Aquila (Apennines) and 0.49 g, which is the maximum value, for the municipality of Laino Castello (Cosenza), as it is located right on the Calabrian arch. In contrast, municipalities and cities located outside such areas have lower expected PGA values. This is, for example, the case for Milan, with a PGA equal to only 0.06 g, Gallarate (Varese) with a PGA of 0.04 g and Cagliari with PGA of 0.05 g (Colombi et al. 2010).

Studies of historical earthquakes show that seismic events often occur in areas that have already been hit in the past. Furthermore, expected event typologies in Italy are similar, due to the trigger sources, which are focal mechanisms that are particularly related to dip-slip (normal and reverse) faults. As a consequence, it makes sense to develop a predictive relationship based on this type of information.

An analysis to establish the ground motion–damage relationship, which accounts for diverse structure types, can only be performed in places where building census and vulnerability data are available or can be easily inferred for each structural scheme (Jaiswal and Wald 2013).

Consequently, as a second source, data about the population and construction materials of existing residential buildings is required. Indeed, it is fundamental to know the exposure of a studied area, the age of its buildings, and the materials used to construct them.

Such information is essential when it comes to evaluating the exposure, and then also the vulnerability, of the built environment according to the performance-based earthquake engineering (PBEE) approach (Goulet et al. 2007). PBEE is based on the definition of rigorously scientific performance metrics, which are relevant to decision making for seismic risk mitigation and reflect economic losses, functionality loss and risk of casualties (Deierlein et al. 2003). A major study in this field is that from Deierelein et al. (2003), that developed the performance assessment equation, based on the probabilistic combination of four generalized variables: decision variable, damage measure, engineering demand parameter and intensity measure.

In this paper, the main assumption is made by assessing expected seismic losses as against actual national exposure. The Italian building stock is modelled in this paper by also accounting for its spatial distribution with respect to each municipality according to the 14th census database of the National Institute of Statistics (ISTAT 2011). The database accounts for the number of residential buildings in each municipality, their diverse construction materials (reinforced concrete, masonry or mixed buildings), and the age of construction, i.e. seismically or non-seismically designed.

The vulnerability of the Italian building stock is also evaluated through the implementation of seismic fragility curves. These define the fragility of buildings in terms of the structural limit state probability of exceedance as a function of an intensity measure (IM) of an earthquake. In the present study, a set of fragility curves from the literature is used with respect to the PGA. Several studies from the literature were also investigated, with those that refer to typical European structural typologies selected for this paper (Ahmad et al. 2011; Borzi et al. 2007, 2008; Crowley et al. 2008; Erberik 2008; Kappos et al. 2003, 2006; Kostov et al. 2004; Kwon and Elnashai 2006; Lagomarsino and Giovinazzi 2006; Ozmen et al. 2010; Rota et al. 2010; Spence 2007; Tsionis et al. 2011).

The curves are selected by also referring to the structural typologies, which are identified from the ISTAT dataset (ISTAT 2011). As a result, vulnerability is evaluated for seismically and non-seismically reinforced concrete buildings, non-seismically designed masonry buildings, and seismically and non-seismically constructed mixed buildings.

Fragility curves, which classify residential buildings according to the examined diverse structural typologies, are used, while, on the basis of the PGA, the probability of exceedance of the limit state *ls* is provided by Eq. (1) as follows:

$$P[LS = ls/PGA] = F_{LS,i}(PGA) - F_{LS+1,i}(PGA) \quad \text{with} \quad 1 \leq ls \leq j \tag{1}$$

with each set of curves averaged for each building typology, *i*.

2.2 Earthquake scenario analysis: accounting for seismic ground shaking correlations

Earthquake scenarios are generated through statistical simulations of historical events. In particular, a normal distribution is used to describe the probability distribution for the intensity measure given the various ground motion source and path parameters, which is obtained in each municipality for each earthquake. The PGA is used as the intensity parameter, the values of which are calculated according to the attenuation law of Bindi et al. (2009). It is in fact possible to consider a single ground-motion parameter, as is the

case in many ground-motion prediction equations (GMPE). Such a univariate approach is advocated as it regards ground-motion parameters as almost multivariate log-normal variables (Goda and Atkinson 2009).

The GMPE of Bindi et al. (2009) adopts the same functional form as the formula from Sabetta and Pugliese (1996), but updates its coefficients, as shown in Eq. (2):

$$\log_{10}(PGA) = -1.344 + 0.328 \cdot M - \log_{10}\sqrt{(R^2 + h^2)} + 0.262 S_i \pm \sigma \qquad (2)$$

The ground motion prediction equation (GMPE) from Bindi et al. (2009) enables to assess the mean of the logs of PGA for each seismic event and for the barycentre of each Italian municipality. Hence, using this GMPE means that for each magnitude level a normal multivariate PGA field is considered. Furthermore, the relationship from Bindi et al. enables to distinguish the intra-event and the inter-event residual, which are typically assumed to be independent and normally distributed. Keeping with this, errors associated to the assessed PGA values are generated to derive the acceleration field associated to each historical event. Errors generated have a normal multivariate distribution too. In fact, they are drawn with the median equal to the value attained from the attenuation law and covariance matrix, $\sum$, equal to that shown in Figs. 5 or in 6, depending on the considered limit case.

Some assumptions are made in the context of the present study: M is assumed to be equal to Msp, which is the corrected magnitude according to Sabetta and Pugliese (1996), and is also provided by the INGV catalogue; and R is taken to be the epicentral distance from the centre of each municipality (km). For municipalities less than 5 km from an epicentre, the PGA is assumed to be equal to the epicentre. Meanwhile, for municipalities greater than 100 km from an epicentre, the PGA is assumed to be zero.

In this first step, S_i is assumed to be zero, which means that the PGA is evaluated by making assumptions about rock soil conditions. Meanwhile, σ is the standard deviation of the log of the PGA and is provided by Eq. (2) as follows:

$$\Sigma = \sigma^2 \begin{bmatrix} 1 & 0 & \cdots & \cdots & 0 \\ 0 & \ddots & & & 0 \\ \vdots & & 1 & & \vdots \\ \vdots & & & \ddots & \vdots \\ 0 & \cdots & \cdots & 0 & 1 \end{bmatrix}_{8101X8101}$$

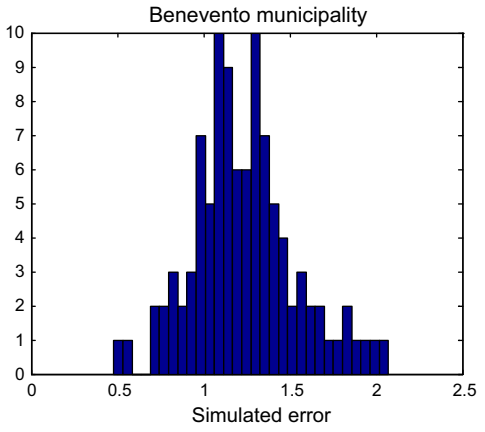

Fig. 5 Error simulated (Nsim = 100) for Molise 2002 (Msp = 5.59) for the Benevento municipality in the case of the fully uncorrelated PGA

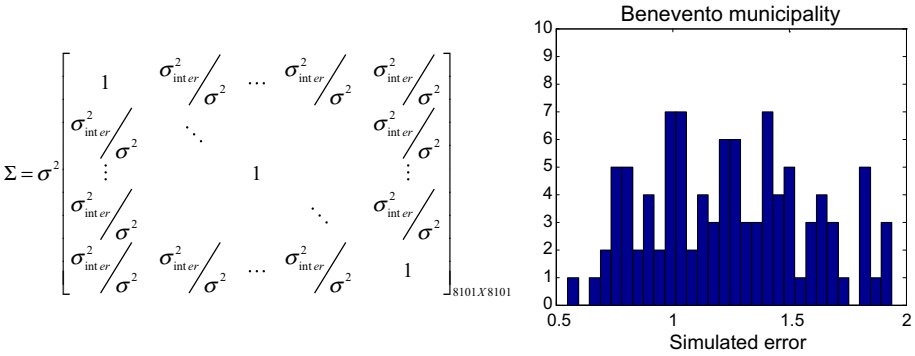

Fig. 6 Error simulated (Nsim = 100) for Molise 2002 (Msp = 5.59) for the Benevento municipality in the case of the partially correlated PGA

$$\sigma^2 = \sigma_{\text{inter}}^2 + \sigma_{\text{intra}}^2 = (0.174)^2 + (0.222)^2 \tag{3}$$

where σ_{inter} is the inter-event standard deviation and σ_{intra} the intra-event standard deviation.

When dealing with the simulation of earthquake scenarios, the inter- and intra-event variability must be taken into account, especially when considering spatially distributed systems such as a residential portfolio. Spatially distributed systems are in fact exposed to simultaneous excitations when an earthquake occurs. Accordingly, the correlation between seismic effects is very important when assessing seismic losses, because it can potentially affect the probability distribution of seismic damage (Hong et al. 2009).

In particular, inter-event variability is also known as earthquake-to-earthquake variability and emphasizes the correlation between registrations of different earthquakes at the same site. Meanwhile, intra-event variability, i.e. the alleged site-to-site variability, indicates the variation of seismic excitations for a particular earthquake from site to site (Goda and Hong 2008b).

Inter- and intra-event variability is dependent on ground-motion parameters, although the latter is also a function of the distance between two sites. The interrelation between the ground motion parameters from site to site could have a major impact on the results obtained by the GMPE at short separation distances, due to saturation effects (Goda and Atkinson 2010). This is certainly true for distances up to 1 km, since the degree of correlation decreases with the increasing distance between two sites (Goda and Hong 2008a). In view of this, it must be taken into account that the current study uses a full-scale approach to the Italian peninsula, where the separation distance is evaluated between municipalities with a mean distance of over 10 km from each other. As a consequence, in order to properly take into account the correlation, only the inter-event element was considered, as seismic losses could otherwise be overestimated, leading to excessively cautious evaluations (Hong 2000).

On the basis of such considerations, two limit cases are investigated to evaluate the differences obtained in the evaluation of expected losses when performing scenario simulations. The cases modelled are: a completely uncorrelated PGA, in which $\sigma = \sigma$, i.e. the total correlation in the residuals of the ground motion prediction equation is computed; and a partially correlated PGA, in which only the inter-event correlation is considered.

This could be achieved because inter- and intra-event correlations are usually considered to be independent, and could therefore be studied separately (Goda and Hong 2008b).

In both the fully uncorrelated and partially correlated PGA cases, error simulation according to a multivariate normal distribution is performed, with a median equal to the PGA calculated according to the attenuation law of Bindi et al. (2009). Consequently, on the basis of this law, 100 values of the residuals are randomly extracted for each simulated earthquake for each Italian municipality.

Error simulation is performed by defining the covariance matrix (assuming that it is normally distributed) with a zero mean and a covariance matrix Σ, which varied depending on the case being examined. So, in the case of the completely uncorrelated PGA, it accounted for the total standard deviation provided by Bindi et al. (2009). This is while it only accounted for the inter-event allocated share in the case of the partially correlated PGA. In this case, the main diagonal elements account for the total standard deviation, while off-diagonal ones account only for the inter-event standard deviation.

Figures 5 and 6 set out the adopted covariance matrixes in the two studied limit cases, together with the related trends of the residuals.

In the case of fully uncorrelated PGA, an $N \times N$ matrix with unit diagonal term and zero off-diagonals is obtained, where N was the number of Italian municipalities.

In the inter-event correlation case, the resulting correlation between the residuals is accounted for through the incorporation of the spatial correlation model in the covariance matrix that is associated with inter-event variability.

The results in terms of the frequency of the residuals show a clear log-normal trend, which is more scattered in the case of the uncorrelated than the inter-event correlated assumption. Such an observation can be justified by the major interrelation accounted for in the second case, which makes the residuals obtained more similar.

Once the PGA field is derived from each earthquake, it is evaluated for the entire Italian territory (assuming rock soil type). The PGA values are then amplified according to the topographical and stratigraphic coefficient of each municipality, as defined by the INGV (2004) report.

2.3 Expected losses against spatial correlation

Direct economic losses are computed by implementing a discrete version of the PBEE equation set out in Asprone et al. (2013) and shown in Eq. (4) as follows:

$$l_i = \sum_{LS=1}^{n} RC(LS) \cdot [P(LS|\overline{\mathrm{PGA}}) - P(LS+1\,|\overline{\mathrm{PGA}})] \quad [€/\mathrm{sqm}] \tag{4}$$

where l_i represents the specific expected loss, i.e. per square meter of residential units i, $RC(LS)$ is the restoration/reconstruction cost function, and $\overline{\mathrm{PGA}}$ is the earthquake IM evaluated for each municipality through the attenuation law and then amplified for the stratigraphic and topographical coefficients S_S and S_T. The PGA value also takes into account the respective error in the two cases of the completely uncorrelated and partially correlated PGAs.

The term $[P(LS|\overline{\mathrm{PGA}}) - P(LS+1|\overline{\mathrm{PGA}})]$ represents the probability of exceedance of the limit state given the particular PGA within each discrete set considered.

Fragility curves are selected from the literature, to evaluate such a probability for masonry and r.c. buildings, as done in Asprone et al. (2013).

The results in terms of the expected economic loss per square meter are averaged for each fragility curve considered and each structural scheme, according to the age of construction. Mean values are then integrated on the entire square meters amount and summed up for all the municipalities in order to compute the total national loss for each simulated earthquake, L_m.

The seismic retrofitting or reconstruction unit costs are also included in the loss curve derivation in this step for the diverse structural typologies. The reconstruction cost per square meter when the collapse limit state is attained is assumed to be equal to 1,500 €/sqm according to information from the Italian Centre for Sociological, Economics and Market Research (CRESME 2011).

Consequently, according to the study by Asprone et al. (2013), the repair costs are expressed as a function of the reconstruction cost $RC_{collapse}$. Moreover, they are assumed to have a linear trend against the limit states i for each vulnerability curve, as shown by Eq. (5).

$$RC(LS) = \left(\frac{i}{n}\right) \cdot RC_{collapse} \tag{5}$$

The presented relationship allowed to also evaluate the unit loss for intermediate limit states and to retain this invariant for the assumptions made. It also ensured adequate flexibility with respect to the set of discrete limit states, which had a different number of damage state levels n for each investigated fragility curve study. Fragility curves and the related limit states, damage level and number, are the same as selected in Asprone et al. (2013).

Expected national losses are evaluated for each earthquake simulation performed and then plotted against the magnitude of Sabetta and Pugliese, as provided by the INGV catalogue (2004) in the cases of the fully uncorrelated PGA (Fig. 7) and the inter-event PGA correlation (Fig. 8).

Experimental evidence revealed a more concentrated distribution of total losses in the case of the fully correlated PGA, as expected. As a further assumption, the PGA is computed for the centroid of each municipality, and is considered to be uniform across the entire municipality. Figure 9 below demonstrates the distribution of loss values for the

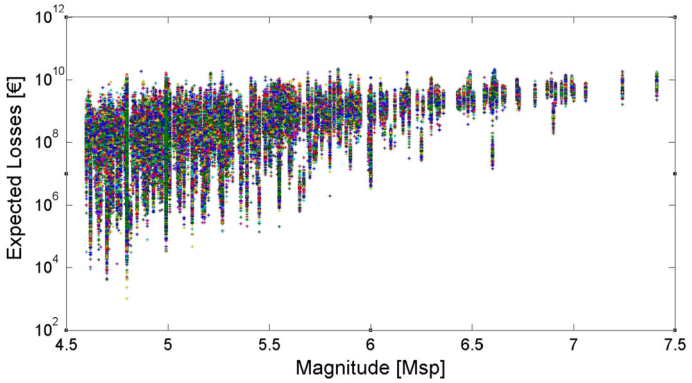

Fig. 7 Total expected losses for each simulated earthquake in the case of the fully completely uncorrelated PGA

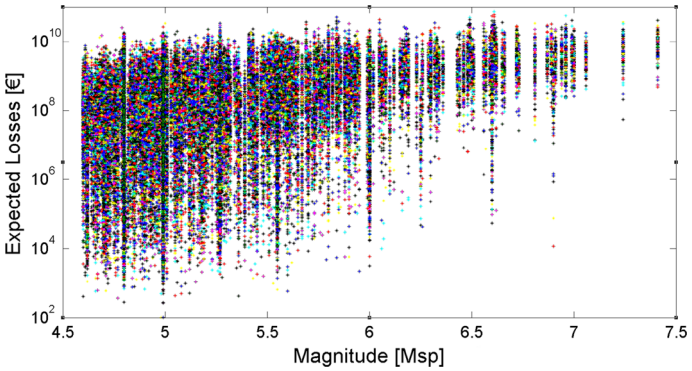

Fig. 8 Total expected losses for each simulated earthquake in the case of the partially correlated PGA

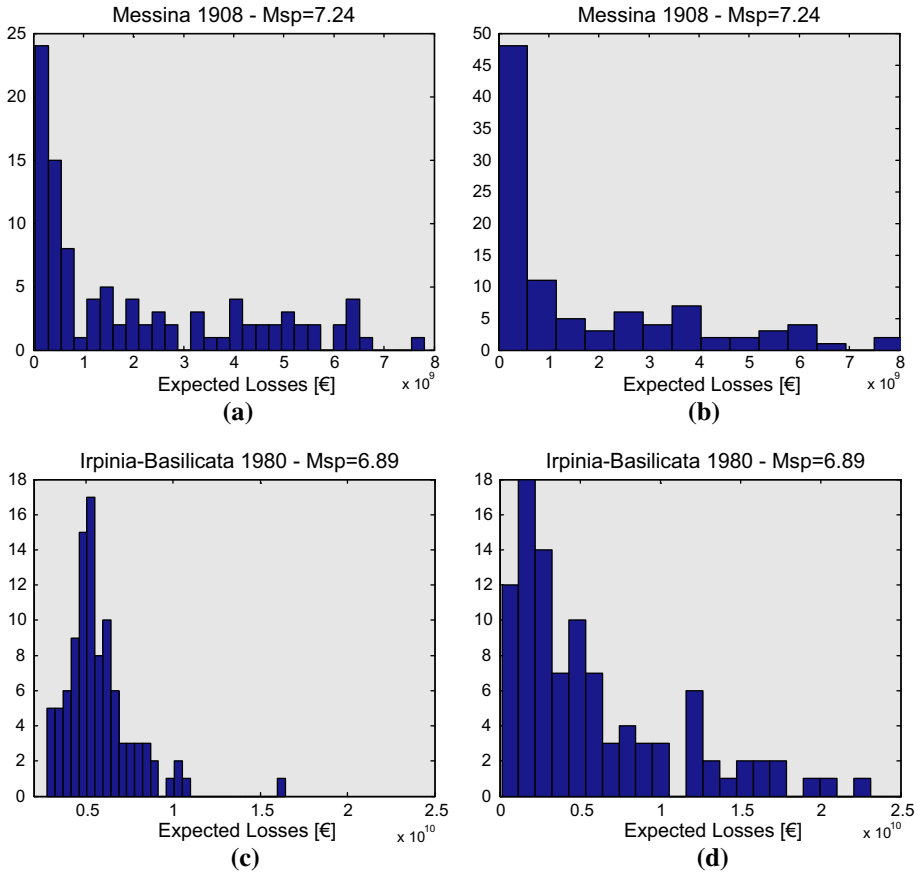

Fig. 9 Expected losses for the Italian peninsula evaluated in the cases of the fully uncorrelated (*left side*) and the partially correlated assumptions (*right side*). The results refer to the historical seismic events in Messina in 1908 (**a**, **b**) and Irpinia in 1980 (**c**, **d**)

events of Messina 1908 and Irpinia 1980 based on the assumption of fully uncorrelated and partially correlated PGA values.

The results show the sensitivity of the annual expected loss (AEL) to different correlation cases, although it is often not recommended, as it could fail to capture the extent of the loss distribution, especially when dealing with rare events (Yoshikawa and Goda 2013).

As the proposed methodology would help the insurance market to mitigate the risk of insolvencies, with the objective being to estimate expected losses as realistically as possible, adopting AEL as a scalar risk metric seems to be appropriate. Insurers in fact mostly assess possible solutions and actions based on financial and monetary indicators. Moreover, the proposed approach allows us to adopt a risk-neutral approach, which is fundamental as it is very difficult to evaluate the actual behaviour of the stakeholders involved. This is because of the willingness of private householders to potentially buy insurance being not affected by changes in the expected losses values. With this, expected prices estimated by the insurer, according to the proposed procedure, may be assumed to be pretty the same of the real ones to be potentially required on the market.

3 Processing the results of the analysis

Spatial modelling of the ground motion for each municipality allows to take into account the spatial distribution of the residential building system in Italy. Doing this enables to perform the scenario simulation according to the joint distribution of ground motion parameters at different sites.

The right spatial tail of the loss distribution can also be assessed according to the local exposure and the annual ground motion rate.

The results demonstrate more scatter in terms of expected losses based on magnitude for the partially correlated than the uncorrelated PGA case. An example is the 1873 earthquake in Venafro, which had an Msp = 4.99, with statistics on the event's assessed loss values confirming the observed trend.

As expected, it can be seen (Table 1) that the mean loss values are almost equal in the two PGA cases, but the partially correlated case shows significantly greater dispersion.

3.1 Derivation of expected loss relationships through regression analysis

Once the scenario simulations are run, a simplistic linear regression model is used to process results. Clearly, magnitude alone cannot describe perfectly the total expected direct losses. Nevertheless, the simple regression model proposed fits the data fairly well. Accordingly, this technique can be effective in processing expected seismic losses vis-a-vis magnitude.

Table 1 Statistics on the expected losses for the Venafro seismic event

Venafro 1873	PGA fully uncorrelated (€)	PGA partially correlated (€)
Mean	1.06e+009	9.37e+008
Standard deviation	5.71e+008	1.22e+009

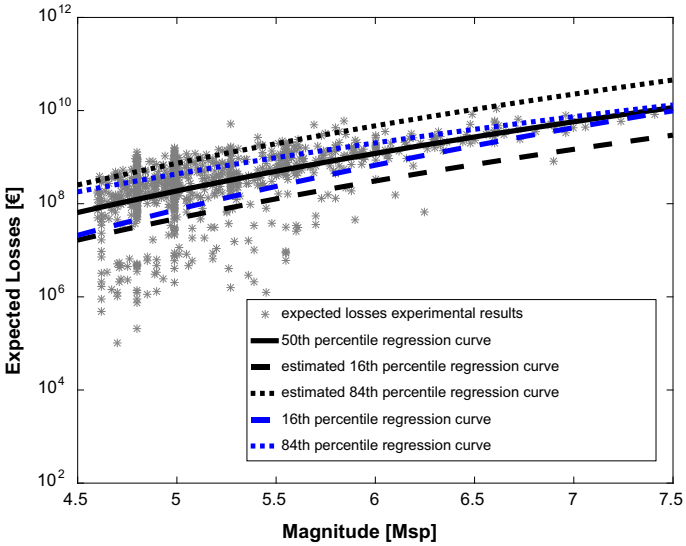

Fig. 10 Expected losses data points and regression curves for the case of the fully uncorrelated PGA

The values of the magnitudes are fixed within the study, because of the deterministic nature of the event being simulated. Starting with magnitude, losses are generated from randomly-generated variables, i.e. the residuals.

A logarithmic regression of the 50th percentile of the estimated losses L^{50th} for both limit cases is performed, and the regression curve is fitted in the semi-logarithmic plane. Consequently, the equation of the regression curve is as follows:

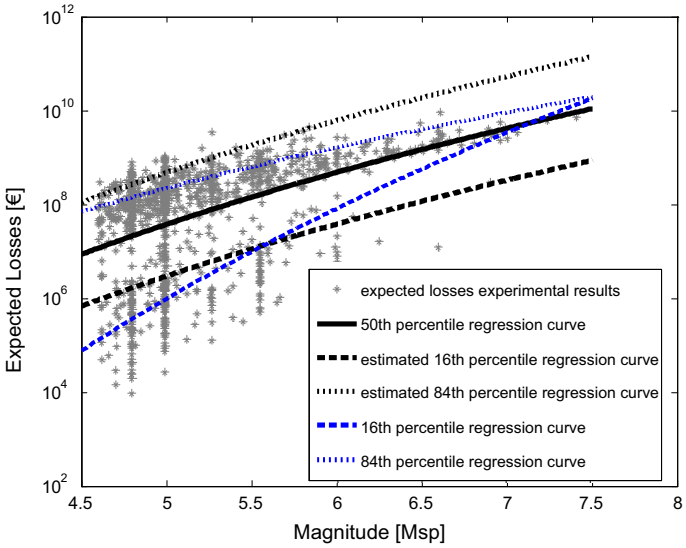

Fig. 11 Expected losses data points and regression curves for the case of the inter-event correlated PGA

$$\log_{10} L^{50\text{th}} = \log_{10} a + b \cdot \log_{10} M_{sp} \tag{6}$$

with $\log_{10}a$ and b being the intercept and slope of the regression curve, respectively. A logarithmic linear regression is then performed, also on the basis of the 16th and 84th percentile values for both the complete and partial PGA correlation cases.

The predictive model for expected loss against the magnitude is shown in Fig. 10 for the fully uncorrelated PGA case and in Fig. 11 for the inter-event correlated PGA case.

Regression can also be understood as a probabilistic model for the distribution of residuals in order to define the probability distribution of L|M, where the homoscedasticity assumption subsists.

Consequently, by assuming constant dispersion, the regression curves for the 16th and 84th percentiles of the loss are estimated in the case of full uncorrelation between PGAs. Starting from the regression curve drawn from the median loss values, these curves can be obtained by simply summing up and subtracting the logarithmic standard deviation [obtained from Eq. (7)] to the regression curve.

$$\sigma \approx s = \sqrt{\frac{\sum_{i=1}^{n} e_i^2}{n-2}} \tag{7}$$

Furthermore it is possible to observe variations in the variance, by assessing the coefficient of determination R^2, according to Eq. (8):

$$R^2 = \frac{\sum_{i=1}^{n} (\hat{y}_i - \bar{\hat{y}})^2}{\sum_{i=1}^{n} (y_i - \bar{y})^2} = 1 - \frac{\sum_{i=1}^{n} [y_i - (ax_i + b)]^2}{\sum_{i=1}^{n} (y_i - \bar{y})^2} \tag{8}$$

that is the complement to the ratio between the residual sum of squares of the set n of data points and the sums of squares of these. Being respectively: $\hat{y}_i$, the logarithm of observed values; $\bar{\hat{y}}$, the logarithm of the mean of theoretical values; y_i, the logarithm of the 100 loss values simulated for each seismic event; and, $\bar{y}$, the logarithm of the mean of 100 simulated loss values.

The coefficient of regression shows how well the sample regression line fits the data. Particularly, it represents the variability of the dependent variable with reference to the independent variable. R^2 is defined in [0,1], being $R^2 \approx 1$ in case perfect fit is achieved, while $R^2 \approx 0$ in case of poor fit.

Figure 10 shows the trend for the 50th, 16th and 84th percentile regression curves, which are depicted with black dots, whose parameters are shown in Table 2, following.

It is clearly evident that for higher magnitudes the 16th and 84th percentile curves tend towards the median (the central one). This is due to the smaller number of historical high magnitude events, as also shown by the data points.

Table 2 Parameters of the 16°, 50° and 84° percentile regression curves in case full uncorrelation is assumed

Regression	$\log_{10}$ a	b	σ	R^2
16° percentile	−0.54	12.05	0.59	0.980
50° percentile	1.19	10.16	0.59	0.983
84° percentile	2.78	8.41	0.59	0.983

Table 3 Parameters of the 16°, 50° and 84° percentile regression curves in case partial uncorrelation is assumed

Regression	In a	b	σ	R^2
16° percentile	−7.24	19.77	0.74	0.994
50° percentile	−0.02	11.44	0.74	0.998
84° percentile	2.52	8.84	0.74	0.999

Meanwhile, in the case in which 16th and 18th percentile curves are estimated from the median (the black lines) curve, the confidence interval remains constant, because of the underlying homoscedasticity.

The same procedure is also performed for empirical data obtained when the scenario analysis is conducted assuming inter-event correlation (Fig. 11).

Table 3 following shows the parameters of the regression curves.

Results similar to those of the uncorrelated PGA case are also observed in the inter-event correlation case. In the case of the homoscedasticity assumption, a similar confidence interval is observed between the median curve and the 16th and 84th percentile curves. On the other hand, in the uncorrelated case assumption, there is greater consistency between the curves. Meanwhile, in Fig. 11, there is less correspondence between the median curve and the 16th percentile regression curve due to the larger dispersion.

In both the case analysis, the fit seems to work quite well for large-magnitude events. However, it can be observed that the data shows more variability around the regression line for low-magnitude events. This in part can be attributed to the fact that for a low magnitude bin, the historical catalogue has a much larger number of events. Therefore, the variability in both vulnerability and exposure characteristics is seen more clearly for low-magnitude events.

Therefore, in the paper, two predictive models are presented: (1) the simple regression with fixed standard error (homoscedastic regression); (2) the simple regression with variable standard error. In the second case, the plus/minus standard deviation confidence interval (in the logarithmic scale) has been evaluated by fitting two regression lines (using the same simple regression fit) to the 16th and 84th percentile total loss estimates calculated from the data. Clearly, the second model is more faithful to the data.

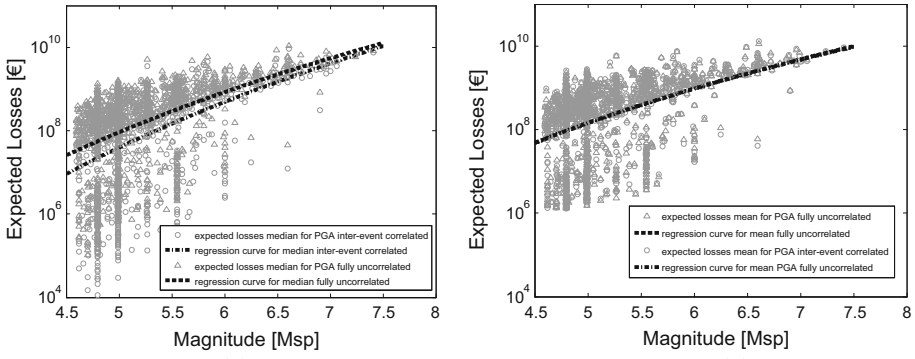

Fig. 12 Regression curves fitted to the median (**a**) and the mean (**b**) in the two cases

Paralleling this, goodness of fit can be assessed by comparing values obtained for the coefficient of determination in the two case analysis. Higher correlation is observed in case inter-event correlation is assumed, $R^2 \approx 0.99$, with respect to the full uncorrelation assumption case analysis, $R^2 \approx 0.98$. Consequently, it can be argued that no error occurs when neglecting error related to the intra-event correlation when dealing with seismic event distributed at the national level, as in Italy.

The percentile curves are derived from both homoscedastic regression and by also directly calculating the 16th and 84th percentiles from experimental data.

The figures below show the regression curves fitted to the median (Fig. 12a) and the mean values (Fig. 12b) of the calculated expected losses for the two cases of uncorrelated (dashed dot) and partially correlated (dashed) PGA values.

The correspondence between the predictive relationships for the two cases when they are fitted to the mean value is perfect. Diversely, the median values for the partially correlated case are lower than for the fully uncorrelated case. This is reasonable, as the partially correlated case is associated with higher standard deviations, meaning that the median must be smaller so that the expected values are equal. Accordingly, as already expected, the analysis of the results in terms of the median values shows that, based on the uncorrelated case assumption, the predictive relationship would be very conservative due to an overestimation of seismic losses.

3.2 Bin processing of the empirical results

The number of historical earthquakes is not uniformly distributed within the INGV catalogue (2004). This is because of the intrinsically random nature of earthquake occurrences. The logarithmic regression based on the homoscedasticity assumption cannot capture the smaller number of historical earthquakes, for very large magnitude events.

There are, in fact, a larger number of lower magnitude seismic events, as depicted in Fig. 13 (as also expressed in the Gutenberg–Richter relation).

It can be seen that the rate of occurrence of earthquakes falls as the magnitude rises. This is also reflected in the fact that there are fewer faults that are physically capable of causing very high-magnitude events.

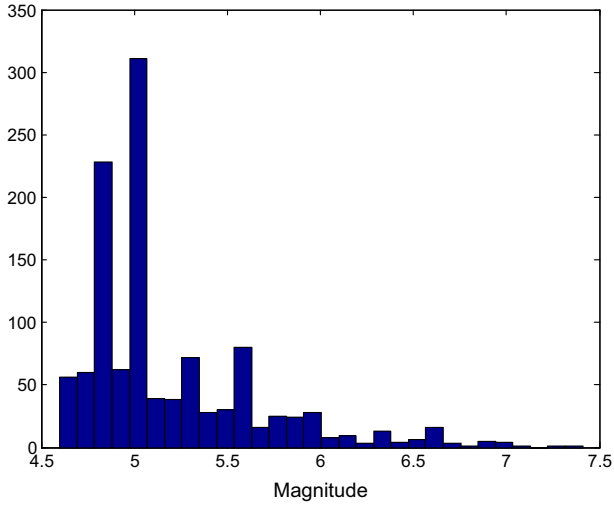

Fig. 13 Frequency of historical earthquakes in terms of magnitude

Table 4 Historical earthquakes for which the scenario analysis is performed, gathered in bins with a 0.10 M amplitude

Bin	N° events	Event interval	
4.6:4.7	56	1	56
4.71:4.81	189	57	245
4.82:4.92	54	246	299
4.93:5.03	243	300	542
5.04:5.14	47	543	589
5.15:5.25	41	590	630
5.26:5.36	67	631	697
5.37:5.47	26	698	723
5,48:5.58	62	724	785
5.59:5,69	29	786	814
5.70:5.80	29	815	843
5.81:5.91	24	844	867
5.92:6.02	21	868	888
6.03:6.13	9	889	897
6.14:6.24	8	898	905
6.25:6.35	14	906	919
6.36:6.46	5	920	924
6.47:6.57	6	925	930
6.58:6.68	14	931	944
6.69:7.05	13	945	957
7.06:7.42	3	958	960
	960		

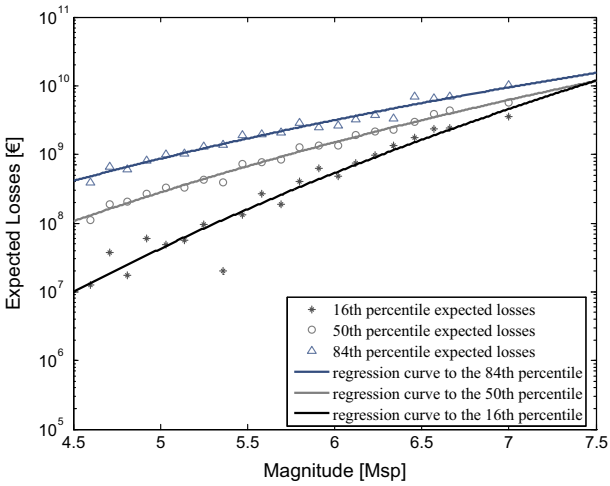

Fig. 14 Bin regression in the case of the fully uncorrelated assumption

A total of 1172 events are listed in the INGV catalogue, but some of these have their epicentre's location close to the borders of the country or deep in the Tyrrhenian Sea. Obviously, the expected seismic damage from such events is slight, and accounting for

them may thus produce an unjustified shift of the prediction curve. To avoid such a phenomenon, events with the epicentre in these areas are removed from the catalogue. Accordingly, 960 instead of 1172 earthquakes are simulated.

Furthermore, to account for the diverse distribution of the number of earthquakes against the magnitude, historical events are grouped in bins, and expected losses are computed for each of them (Table 4).

A bin width of 0.10 M is used to group the expected loss data in order to perform the regression analysis. A greater width—equal to 0.36 M—is assumed for the last two bins, being empty the magnitude intervals 7.07:7.23 and 7.25:7.40.

A logarithmic regression analysis is again performed for the 16th, median and 84th percentiles of loss according to the least squares method. The results are shown in Figs. 14 and 15, as follows.

As expected, lesser data points can be observed, and reflect the expected loss assessment based on the bin division according to the magnitude intervals (Fig. 16).

The regression curves show similar trends for the fully uncorrelated and partially correlated PGAs. Nonetheless, due to the wider distribution of the data points in the case of the inter-event correlation assumption, major scatter is detected.

3.3 Comparisons and results

The assumption of the fully uncorrelated PGA clearly leads to a steeper regression curve and a smaller confidence interval. On the other hand, the partially correlated PGA values are more scattered and, as a consequence, the confidence intervals around the regression curve are wider.

The most of the difference in the distribution provided by the two simulation cases is due to the standard deviation values.

In the case of fully uncorrelated simulations, where no spatial correlation is taken into account, the loss values demonstrate less scatter, as expected.

Logarithmic regression curves fitted to the mean values coincide in the two cases, as they also do in the case of bin regression. The regression curve to the median instead has

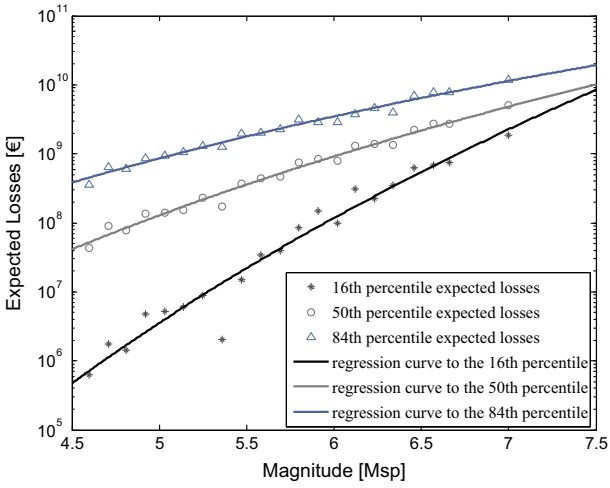

Fig. 15 Bin regression in the case of the partial correlation assumption

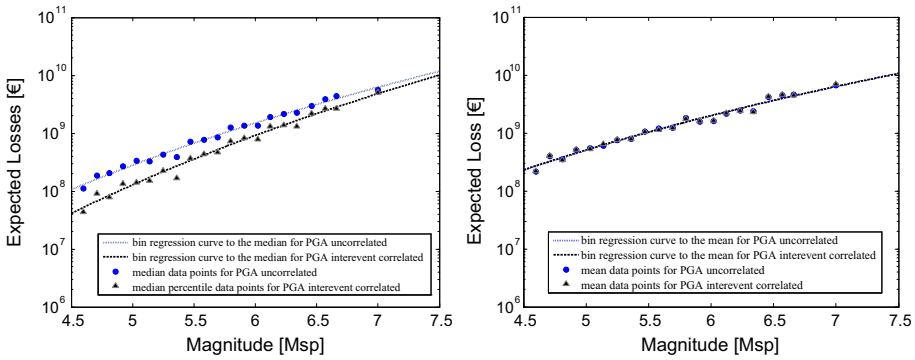

Fig. 16 Regression curves for the median (*left side*) and the mean (*right side*) values for the two limit cases

higher values in the case of the fully uncorrelation assumption, as is also in the case of simple linear regression previously implemented without performing bin division.

As a result, more conservative predictions are produced according to the regression analysis used in the fully uncorrelated PGA hypothesis. Otherwise, lower expected losses are estimated in the case of inter-event correlation, thereby one can expect that a lower margin of safety is attained, allowing for a more realistic evaluation. The experimental observations are also confirmed by studying the size order of the intercept of the plotted curves. According to the median values, at a 4.5 magnitude, about 8.2e+08 € seismic losses are expected in the case of the fully uncorrelated PGA and 5e+07 € in the case of the correlated PGA inter-event.

Further remarks are related to the differences between the case in which a regression analysis is performed according to the bin division and one according to each magnitude (Msp) value. The regression curves are set out in Fig. 17 for the fully uncorrelated assumption.

The expected loss in the case in which the regression analysis is performed according to the bin division provides higher loss values than the regression case implemented for each Msp value. Performing the regression to the median or the mean values by considering the

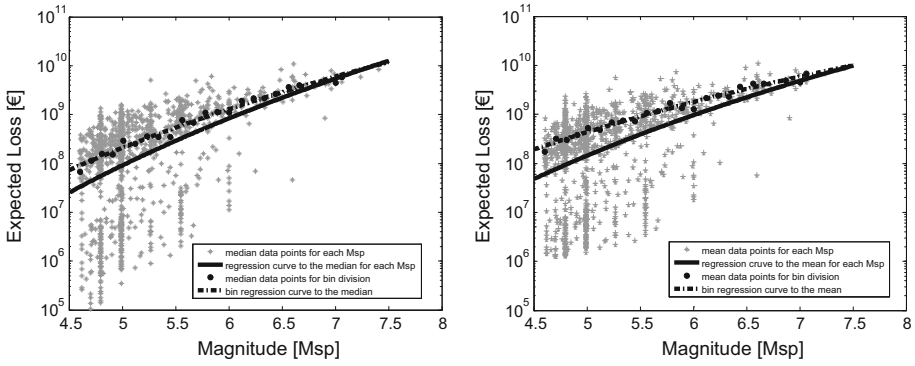

Fig. 17 Case of the fully uncorrelated PGA: comparison between the regression curves of the median (*left side*) and the mean values (*right side*) in the case of bin regression and the case of regression for each magnitude (Msp) value

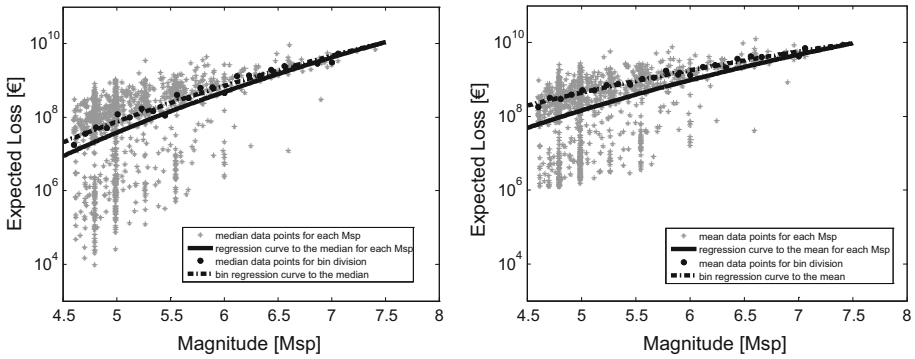

Fig. 18 Case of inter-event correlated PGA: comparison between the regression curves for the median (*left side*) and the mean values (*right side*) in the bin regression case and the case of regression for each magnitude (Msp) value

Table 5 Comparison between the mean and median values calculated in the case of the scenario analysis performed according to the fully uncorrelated and inter-event correlation assumptions

Case analysis	Bin		Msp values	
	Mean (μ)	Median (η)	Mean (μ)	Median (η)
PGA fully uncorrelated	2.01e+09	1.09e+09	8.44e+08	3.29e+08
PGA inter-event correlated	1.99e+09	4.48e+08	8.51e+08	1.88e+08

real loss distribution for each magnitude value allows to forecast more realistic seismic losses.

The precision observed in the case of the regression for each Msp value can also be understood in the sense of a better evaluation of the actual loss distribution given the magnitude. Greater scatter between the regression curves obtained respectively in the case of the bin division and in the case of the simple regression performed for each magnitude value, in fact, can be observed when referring to the mean loss values.

There are similar results when the inter-event correlated PGA is observed for the two kinds of regression (Fig. 18).

It can be seen that the dotted curves—referring to the bin regression case—are also higher in the case of the inter-event correlation assumption. Furthermore, the scatter between the curve related to the bin regression and the curve according to the single Msp values is less in the case of the regression curve fitted to the median.

Some common features can be observed with reference to the scatter trend between the curves in the bin and Msp value regression cases. The scatter is greater for lower magnitudes and tends to zero for higher ones. This is obviously due to the lesser number of rare events.

The major effectiveness of using the Msp regression curves with respect to the median values is also confirmed by the difference between the mean and median values, as calculated in the two limit cases (Table 5).

The results show diverse scattering between the curves fitted to the two limit cases when the bin or Msp regression is performed. A slight drop is observed in both cases with reference to the mean values. In particular, in the case of the Msp regression analysis, only about a 1% drop from the inter-event PGA case with respect to the uncorrelated PGA is

evaluated. In the case of the bin regression, a 4.5% drop is observed from the inter-event to the uncorrelated case.

On the other hand, substantial differences are assessed in the case in which the median values are considered; 9.54 and 42.42% increases are evaluated for the bin regression and Msp regression cases, respectively.

4 Conclusions

Seismic insurance is a potential tool for risk mitigation, although the modelling currently used is a matter of great concern. On the insurers' side, a deep knowledge of exposed goods and site-specific hazards is a major requirement. The main issue that insurers have to face when dealing with private seismic insurance concerns the knowledge needed of effective economic resources. Indeed, this is fundamental when it comes to the insurers' capacity to both pay the insured without becoming insolvent and cover expenses without having cash flow problems. By collecting information about previous earthquakes (960 events) and the population living in residential buildings today, this study establishes predictive relationships for expected economic losses based on magnitude.

The approach employed for deriving predictive relationships takes into account the spatial correlation in the residuals of the ground motion prediction equation. Such correlations are accounted for within the process by using two limit cases: one where there is a full uncorrelation between the attained PGA values, and another in which there is partial correlation. According to the former hypothesis, the PGA affecting each municipality does not depend on the PGA in an adjacent municipality. Meanwhile, in the case where inter-event standard deviation is considered, a partial correlation is assumed between PGA values. This last hypothesis reveals to be coherent with empirical observations (Goda and Atkinson 2010; Goda and Hong 2008a; Hong 2000). According to these the intra-event correlation between ground motion parameters decrease as the distance from site to site increase. Hence, due to this paper dealing with distances between Italian municipalities, which are quite high (over 10 km), intra-event correlation can be neglected without incurring in significant errors. As a result, variability of results is reduced and the importance of accounting for inter-event correlation is highlighted.

The study proposes a general methodology, which can be potentially applied to diverse fields of interest. Particularly, in authors' view, the insurance pricing can be regarded as one of the most direct application. The proposed methodology can potentially enable to optimize insurers' pricing, by performing an accurate estimates of average losses. In fact, obtaining accurate estimates of average losses is an important factor for establishing the prices of insurance coverages. Expected seismic losses can be assessed according to a side by side comparison between the two limit hypothesis regarding spatial correlation of seismic ground motion. Hence, this gives the chance to an insurance company to perform a prompt loss assessment in a less conservative manner.

Furthermore, the methodology has got the potential to foster interactions among the diverse stakeholders involved in disaster management and recovery processes to be optimized. For instance, experimental evidence shows that a better knowledge of expected losses allows insurers to increase market penetration; a firm can sell insurance at a lower profit margin, as it does not need to prevent insolvency and does not pay as much for reinsurance by relying more on its own reserves (Kesete et al. 2014).

The results are presented in terms of the 16th, median and 84th percentiles for expected loss curves given magnitude based on the two distinct assumptions.

The difference in the distribution produced by the two simulation cases is obvious regarding the standard deviation values. More scatter is actually observed when a scenario analysis is performed in the partial correlation assumption case. Accordingly, when no spatial correlation is taken into account, more aggregated loss values are obtained.

As a consequence, in the case of the partially correlated PGA values with respect to the uncorrelated case, the confidence intervals of the 16th/84th percentiles around the median are higher, in agreement with similar results in the literature (Goulet et al. 2007).

For low probability values, there is a higher scattering of values from the median.

More confidence is given to the regression curves referring to lower magnitude values, due to the high number of historical events.

In general, the predictive relationships derived for expected losses given the magnitude clearly have a significant dependence on how the PGA correlation is modelled. A substantial exception is represented by the curves fitted to the mean, which demonstrates insensitivity to the spatial correlation model. This also confirms (e.g. see Yoshikawa and Goda 2013) that the choice of a suitable risk metric for insurers is extremely important for decision-making.

Further processing of the obtained results in terms of the expected losses is performed. The expected loss values, which are obtained from simulation of the events in the INGV catalogue, are also divided into bins before conducting the regression analysis. The bins were modelled by considering the same amplitude of the interval according to the magnitude of the simulated events. Each bin accounted for a diverse number of historical seismic events, but the same weight is assigned to each of them within the regression analysis.

The results of the logarithmic regression according to the median and mean values are similar to those obtained in the case in which the results are processed according to each single magnitude value (Msp).

In fact, the predictive relationships drawn in the case of regression according to the Msp result are less conservative than in the case of the bin regression analysis. As a result, more realistic forecasting can be expected when referring to the Msp regression, above all with respect to the median curve.

Consequently, major caution is needed both in the case in which full uncorrelation is assumed and also when the predictive relationship is derived from the bin processing of expected losses.

The main strength of the proposed methodology is that it allows for the prompt and easy forecasting of seismic losses given the magnitude of an event. This can be easily integrated into insurers' decision-making processes within an integrated regional catastrophic loss estimation model that accounts for the spatial distribution of buildings at the municipality level. This approach provides an accurate and disaggregated representation of the risk to be managed, including the spatial correlation and variability of the fragility model. Moreover, retro-fit actions can actually be easily integrated within the evaluation process by changing the fragility curves used within the scenario analysis to characterize vulnerability.

References

Ahmad N, Crowley H, Pinho R (2011) Analytical fragility functions for reinforced concrete and masonry buildings aggregates of euro-Mediterranean regions—UPAV methodology. Internal report, Syner-G Project 2009/2012

Asprone D, Jalayer F, Simonelli S, Acconcia A, Prota A, Manfredi G (2013) Seismic insurance model for the Italian residential building stock. Struct Saf 44:70–79
Bindi D, Luzi L, Pacor F, Sabetta F, Massa M (2009) Towards a new reference ground motion prediction equation for Italy: update of the Sabetta–Pugliese (1996). Bull Earthq Eng 7(3):591–608
Borzi B, Pinho R, Crowley H (2007) SP-BELA: Un metodo meccanico per la definizione della vulnerabilità basato su analisi pushover semplificate. In: Proceedings of XII Convegno L'Ingegneria Sismica in Italia ANIDIS 2007, Pisa, Italy **(in Italian)**
Borzi B, Crowley H, Pinho R (2008) The influence of infill panels on vulnerability curves for RC buildings. In: Proceedings of the 14th world conference on earthquake engineering, Beijing, China
Colombi M, Crowley H, Di Capua G, Peppoloni S, Borzi B, Pinho R, Calvi GM (2010) Mappe di rischio sismico a scala nazionale con dati aggiornati sulla pericolosità sismica di base e locale. Progettazione Sismica. http://hdl.handle.net/2122/6524. Accessed 15 March 2016
Crowley H, Borzi B, Pinho R, Colombi M, Onida M (2008) Comparison of two mechanics-based methods for simplified structural analysis in vulnerability assessment. In: Advances in Civil Engineering
CPTI Working Group (2004) Catalogo Parametrico dei Terremoti Italiani, versione 2004 (CPTI04). Istituto Nazionale di Geofisica, Gruppo Nazionale per la Difesa dai Terremoti, Storia Geofisica Ambiente, Servizio Sismico Nazionale. http://emidius.mi.ingv.it/CPTI/. Accessed 10 Jan 2016
CRESME, Fondazione Housing Sociale (2011) Il mercato delle costruzioni 2012. XIX Rapporto Congiunturale e previsionale CRESME. Lo scenario di medio periodo, 2015
Deierlein GG, Krawinkler H, Cornell CA (2003) A framework for performance-based earthquake engineering. In: Pacific conference on earthquake engineering, Christchurch, New Zealand
Erberik MA (2008) Generation of fragility curves for Turkish masonry buildings considering in-plane failure modes. Earthq Eng Struct Dyn 37(3):387–405
Goda K, Atkinson GM (2009) Interperiod dependence of ground-motion prediction equations: a copula perspective. Bull Seismol Soc Am 99(2A):922–927
Goda K, Atkinson GM (2010) Intraevent spatial correlation of ground-motion parameters using SK-net data. Bull Seismol Soc Am 100(6):3055–3067
Goda K, Hong HP (2008a) Estimation of seismic loss for spatially distributed buildings. Earthq Spectra 24(4):889–910
Goda K, Hong HP (2008b) Spatial correlation of peak ground motions and response spectra. Bull Seismol Soc Am 98(1):354–365
Goulet CA, Haselton CB, Mitrani-Reiser J, Beck JL, Deierlein GG, Porter KA, Stewart JP (2007) Evaluation of the seismic performance of a code-conforming reinforced concrete frame building—from seismic hazard to collapse safety and economic losses. Earthq Eng Struct Dyn 36(13):1973–1997
Hong HP (2000) Distribution of structural collapses and optimum reliability for infrequent environmental loads. Struct Saf 22(4):297–311
Hong HP, Zhang Y, Goda K (2009) Effect of spatial correlation on estimated ground-motion prediction equations. Bull Seismol Soc Am 99(2A):928–934
ISTAT 14 (2011) Censimento generale della popolazione e delle abitazioni. http://dawinci.istat.it/MD/dawinciMD.jsp. Accesses 30 Nov 2015
Jaiswal K, Wald DJ (2013) Estimating economic losses from earthquakes using an empirical approach. Earthq Spectra 29(1):309–324
Kappos AJ, Panagiotopoulos C, Panagopoulos G, Papadopoulos E (2003) WP4—Reinforce Concrete Buildings (Level 1 and Level 2 analysis). RISK-UE Technical report
Kappos AJ, Panagopoulos G, Panagiotopoulos C, Penelis G (2006) A hybrid method for the vulnerability assessment of R/C and URM buildings. Bull Earthq Eng 4(4):391–413
Kesete Y, Peng J, Gao Y, Shan X, Davidson RA, Nozick LK, Kruse J (2014) Modeling insurer-homeowner interactions in managing natural disaster risk. Risk Anal 34(6):1040–1055
Kostov M, Vaseva E, Kaneva A, Koleva N, Varbanov G, Stefanov D, Darvarova E, Solakov D, Simeonova S, Cristoskov L (2004) Application to Sofia. RISK-UE Technical report, WP13
Kwon OS, Elnashai A (2006) The effect of material and ground motion uncertainty on the seismic vulnerability curves of RC structure. Eng Struct 28(2):289–303
Lagomarsino S, Giovinazzi S (2006) Macroseismic and mechanical models for the vulnerability and damage assessment of current buildings. Bull Earthq Eng 4(4):415–443
Munich Re, NatCatSERVICE (2011) NATHAN World Map of Natural Hazards, version 2011. Münchener Rückversicherungs-Gesellschaft, Geo Risks Research, NatCatSERVICE
Munich Re, NatCatSERVICE (2015) Loss events worldwide 1980–2014, 10 costliest events ordered by overall losses. Münchener Rückversicherungs-Gesellschaft, Geo Risks Research, NatCatSERVICE

Ordinanza PCM 3519 del 28/04/2006. Criteri generali per l'individuazione delle zone sismiche e per la formazione e l'aggiornamento degli elenchi delle medesime zone, G.U. n.108 del 11/05/2006. http://zonesismiche.mi.ingv.it/. Accessed 30 Nov 2015

Ozmen HB, Inel M, Meral E, Bucakli M (2010) Vulnerability of low and mid-rise reinforced concrete buildings in Turkey. In: Proceedings of the 14th European conference on earthquake engineering, Ohrid, Macedonia

Rota M, Penna A, Magenes G (2010) A methodology for deriving analytical fragility curves for masonry buildings based on stochastic nonlinear analyses. Eng Struct 32(5):1312–1323

Sabetta F, Pugliese A (1996) Estimation of response spectra and simulation of nonstationary earthquake ground motions. Bull Seismol Soc Am 86(2):337–352

Spence R (2007) Earthquake disaster scenario predictions and loss modelling for urban areas. LESSLOSS Technical report 7

Tsionis G, Papailia A, Fardis MN (2011) Analytical fragility functions for reinforced concrete and masonry buildings aggregates of euro-mediterranean regions—UPAT methodology. Internal report, Syner-G Project 2009/2012

Yoshikawa H, Goda K (2013) Financial seismic risk analysis of building portfolios. Nat Hazards Rev 15(2):112–120